ELSEVIER

Signal Processing 80 (2000) 2407–2420

SIGNAL PROCESSING

www.elsevier.nl/locate/sigpro

Behaviour of image degradation model in multiresolution

Sunil K. Kopparapu[a,*], U.B. Desai[b], P. Corke[a]

[a]*CSIRO Manufacturing Science and Technology, PO Box 883, Kenmore, Queensland - 4069, Australia*
[b]*Department of Electrical Engineering, Indian Institute of Technology - Bombay, Powai, Bombay 400 076, India*

Abstract

Multiresolution techniques are being extensively used in signal processing literature. This paper has two parts, in the first part we derive a relationship between the general degradation model ($Y = B \otimes X + W$) at coarse and fine resolutions. In the second part we develop a signal restoration scheme in a multiresolution framework and demonstrate through experiments that the knowledge of the relationship between the degradation model at different resolutions helps in obtaining computationally efficient restoration scheme. © 2000 Elsevier Science B.V. All rights reserved.

Zusammenfassung

Mehrfachauflösungsmethoden werden in der Signalverarbeitungsliteratur häufig verwendet. Dieser Artikel besteht aus zwei Teilen. Im ersten Teil leiten wir eine Beziehung zwischen den Versionen des allgemeinen Degradationsmodells ($Y = B \otimes X + W$) für grobe und feine Auflösungen ab. Im zweiten Teil entwickeln wir eine Methode zur Signalrekonstruktion im Rahmen eines Mehrfachauflösungs-Ansatzes. Weiters zeigen wir mittels Experimenten, daß das Wissen über die Beziehung zwischen unterschiedlichen Auflösungen des Degradationsmodells dazu beiträgt, eine recheneffiziente Signalrekonstruktionsmethode zu erhalten. © 2000 Elsevier Science B.V. All rights reserved.

Résumé

Les techniques multi-résolution sont extensivement utilisées dans la littérature sur le traitment des signaux. Cet article comprend deux parties. Dans la première nous dérivons une relation entre le modèle général de dégradation ($Y = B \otimes X + W$) pour des résolutions grossière et fine. Dans la seconde partie nous développons une technique de restauration de signal dans un cadre multi-résolution et montrons par le biais d'expériences qu'une connaissance de la relation dans le modèle de dégradation à différentes résolutions aide á produire une technique de restauration efficace du point de vue calcul. © 2000 Elsevier Science B.V. All rights reserved.

Keywords: Degradation model; Multiresolution; Signal restoration; Blur and noise removal

1. Introduction

Removal of noise and blur from degraded signals is an important problem addressed in literature for both 1-D [4,5,18,23] and 2-D [12,13,15,25] signals. Estimation of signals degraded by noise and signal capturing

* Corresponding author. Tel.: + 617-3212-4534; fax: + 617-3212-4455.
E-mail address: nil@cat.csiro.au (S.K. Kopparapu).

0165-1684/00/$ - see front matter © 2000 Elsevier Science B.V. All rights reserved.
PII: S0165-1684(00)00128-6

Nomenclature

$\otimes$	circular convolution operator
X	$[X_0, X_1, X_2, \ldots, X_{2^n-1}]^{\mathrm{T}}$
$\underline{X}$	$[X_1, X_2, \ldots, X_{2^n-1}, X_0]^{\mathrm{T}}$ (right shift)
$\underline{\underline{X}}$	$[X_{2^n-1}, X_0, X_1, X_2, \ldots, X_{2^n-2}]^{\mathrm{T}}$ (left shift)
$\overbrace{X, Y}$	$[X_0, Y_0, X_1, Y_1, \ldots, X_{2^n-1}, Y_{2^n-1}]^{\mathrm{T}}$ (Interleaving)
$X\downarrow 2$	$[X_0, X_2, \ldots, X_{(2^n-2)}]^{\mathrm{T}}$ (down sampling)
$X\uparrow 2$	$[X_0, 0, X_1, 0, X_2, \ldots, 0, X_{2^n-1}]^{\mathrm{T}}$ (up sampling)
$C^1_{C^0_W}$	smooth part corresponding to the wavelet transform of C^0_W
$D^1_{C^0_W}$	difference part corresponding to the wavelet transform of C^0_W
$[C^1_{C^0_Y} D^1_{C^0_Y}]$	wavelet transform of C^0_Y
$[C^1_{C^0_X} D^1_{C^0_X}]$	wavelet transform of C^0_X
$[C^1_{C^0_W} D^1_{C^0_W}]$	wavelet transform of C^0_W
B	blur kernel
$\mathscr{B}$	matrix representing the blur kernel
$\mathscr{C}$	matrix representing the undecimated wavelet transform

nonlinearities is an important practical problem addressed richly in literature [14,19,24]. The goal of any signal restoration scheme is to recover the original signal, X, from the observed signal $Y = B \otimes X + W$, degraded by blur (B) and noise (W). In general, it is not possible to find the original signal X exactly and hence in literature we find that an estimate $\hat{X}$ is obtained such that $\hat{X}$ is close to the original signal X in some sense. Tugnait [24] suggests an iterative restoration scheme based on extended Kalman filtering; the solution is made feasible by constraining the solution space. Levy [8] presents a fast quadratic programming algorithm for signal restoration and Sanz et al. [17] give a scheme for restoring time-limited signal which is iterative. There is a thin line dividing the 1-D and 2-D signal restoration literature. Oja et al. [14] suggests a scheme based on parametric projection filter while Alvarez and Mazorra [2] suggest the use shock filters and anisotropic diffusion; these schemes are applicable to both signal and image restoration. Maitre [10] introduces a signal restoration scheme with an aim to restore images. Trussell et al. [23] discuss the solution feasibility issues and more recently Sharma and Trussell [19] give a set-theoretic approach for signal restoration which is based on the error in variables criterion.

Of late multiresolution analysis is being extensively used in the signal processing literature (for example [4,5,11]). Miller [11] presents a wavelet domain algorithm for computing the error-variances associated with signal restoration problem when posed in a MAP estimation framework. Multiresolution is an efficient and effective way of representing data. The data at each resolution is the output of a bandpass filter with some centre frequency and usually the centre frequency of the filters are octave apart [16]. One of the reasons for gain in popularity of multiresolution schemes is due to its ability to produce algorithms which are computationally efficient [9,16]. To build multiresolution schemes requires the knowledge of the behaviour of variable of interest at different resolutions [21]. In this paper, we (i) derive the relationship between the degradation model $Y = B \otimes X + W$ at different resolutions and (ii) show how this information can be used to recover signal degraded by blur (B) and noise (W) in a multiresolution framework. This is the main contribution of this paper. The computational gain of using the suggested multiresolution signal restoration scheme is demonstrated through experiments. The layout of this paper is as follows: in Section 2 we derive the behaviour of the degradation model at various resolutions and give an expression to obtain the model at any resolution given the model at the finest resolution. In Section 3 we show how the model behaviour can be used for signal restoration and also suggest an algorithm for signal restoration. In Section 4 we initially show that the validity of the derivation of the degradation model at different resolutions and then apply it to the problem of signal restoration (both 1-D and 2-D) to substantiate the usefulness of knowing the model behaviour at different resolutions. We conclude in Section 5.

2. Degradation model at different resolutions

In this paper we concentrate on 1-D signal to identify the relationship between the degradation model at different resolutions. The derived relationship is applicable to 2-D images because a 1-D signal can be constructed by stacking the rows of the image. Consider the degradation model at the finest resolution to be given by

$$Y = B \otimes X + W \tag{1}$$

where, $\otimes$ is the convolution operator, Y is the observed signal of finite length 2^n, B is the blur vector of length $2k+1$, W and X are the noise and the original uncorrupted signals, both of length 2^n.

We rewrite (1) using Nomenclature as

$$C_Y^0 = B \otimes C_X^0 + C_W^0 \tag{2}$$

where, $C_Y^0 \stackrel{\text{def}}{=} Y$, $C_X^0 \stackrel{\text{def}}{=} X$, and $C_W^0 \stackrel{\text{def}}{=} W$ and, a superscript "0" represents that the resolution is finest and an increasing sequence of integers represent coarse resolutions (example $C_\bullet^2$ is coarser that $C_\bullet^1$). In the notation introduced earlier we can show (see Appendix A) that the degradation model at one level coarse resolution denoted by superscript "1", can be written as

$$C^1_{C^0_Y} = \left[\left\{ B \otimes \left[\overbrace{C^1_{C^0_X}, C^1_{\overline{C^0_X}}}\right]\right\} \downarrow 2^1\right] + C^1_{C^0_W}, \tag{3}$$

$$D^1_{C^0_Y} = \left[\left\{ B \otimes \left[\overbrace{D^1_{C^0_X}, D^1_{\overline{C^0_X}}}\right]\right\} \downarrow 2^1\right] + D^1_{C^0_W}, \tag{4}$$

where $C^1_{C^0_Y}$ is the smooth part corresponding to the wavelet transform of the sequence C^0_Y, $C^1_{C^0_X}$ is the smooth part corresponding to the wavelet transform of the sequence C^0_X and $C^1_{\overline{C^0_X}}$ wavelet transform of the sequence $\overline{C^0_X}$. As shown in Appendix A, (3) and (4) can be derived by taking the wavelet transform of (2) because the blur producing matrix and the wavelet transform matrix commute. The relationship between the degradation model at the next coarse resolution (denoted by superscript "2"), can be written as

$$C^2_{C^1_{C^0_Y}} = \left[\left\{ B \otimes \left[\overbrace{\overbrace{C^2_{C^1_{C^0_X}}, C^2_{\overline{C^1_{C^0_X}}}}\overbrace{C^2_{C^1_{\overline{C^0_X}}}, C^2_{\overline{C^1_{\overline{C^0_X}}}}}}\right]\right\} \downarrow 2^2\right] + C^2_{C^1_{C^0_W}}, \tag{5}$$

$$D^2_{C^1_{C^0_Y}} = \left[\left\{ B \otimes \left[\overbrace{\overbrace{D^2_{C^1_{C^0_X}}, D^2_{\overline{C^1_{C^0_X}}}}\overbrace{D^2_{C^1_{\overline{C^0_X}}}, D^2_{\overline{C^1_{\overline{C^0_X}}}}}}\right]\right\} \downarrow 2^2\right] + D^2_{C^1_{C^0_W}} \tag{6}$$

and in general, we can write the degradation model at resolution η ($\eta > 0$) given the model at resolution ($\eta - 1$). Suppose the model at resolution ($\eta - 1$) is

$$C^{\eta-1}_{C^{\eta-2}_{\ddots_{C^{1}_{C^{0}_{Y}}}}} = \left[\left\{ B \otimes \left[\overbrace{C^{\eta-1}_{C^{\eta-2}_{\ddots_{C^{1}_{C^{0}_{X}}}}} \cdots \underline{C^{\eta-1}_{C^{\eta-2}_{\ddots_{C^{1}_{C^{0}_{X}}}}}}} \right] \right\} \downarrow 2^{\eta-1} \right] + C^{\eta-1}_{C^{\eta-2}_{\ddots_{C^{1}_{C^{0}_{W}}}}} \tag{7}$$

then at resolution η, we have

$$C^{\eta}_{C^{\eta-1}_{C^{\eta-2}_{\ddots_{C^{1}_{C^{0}_{Y}}}}}} = \left[\left\{ B \otimes \left[\overbrace{\overbrace{C^{\eta}_{C^{\eta-1}_{C^{\eta-2}_{\ddots_{C^{1}_{C^{0}_{X}}}}}} \; \underline{C^{\eta}_{C^{\eta-1}_{C^{\eta-2}_{\ddots_{C^{1}_{C^{0}_{X}}}}}}}} \cdots \overbrace{C^{\eta}_{\underline{C^{\eta-1}_{C^{\eta-2}_{\ddots_{C^{1}_{C^{0}_{X}}}}}}} \; \underline{C^{\eta}_{\underline{C^{\eta-1}_{C^{\eta-2}_{\ddots_{C^{1}_{C^{0}_{X}}}}}}}}}} \right] \right\} \downarrow 2^{\eta} \right] + C^{\eta}_{C^{\eta-1}_{C^{\eta-2}_{\ddots_{C^{1}_{C^{0}_{W}}}}}} \tag{8}$$

Though (8) looks complicated it can be easily constructed provided we observe that to write the model (8) at resolution η we need to replace every element in the inner square parenthesis of (7) appearing at resolution ($\eta - 1$) by the smooth part of the wavelet transform of the element, *interleaved* with the smooth part of the wavelet transform of its *shifted* version. This operation needs to be performed on all elements present in the inner square parenthesis. For example, if C^0_X appears in the model at resolution ($\eta - 1$) then we have

$$\left[\overbrace{C^{1}_{C^{0}_{X}} \; \underline{C^{1}_{\underline{C^{0}_{X}}}}} \right]$$

coming in the expression for the model at resolution η. In addition to this there is a further downsample by a factor of 2 at resolution η. In this sense, construction of the degradation model at different resolutions is straightforward.

3. Application to signal restoration

The problem of signal restoration can be stated as, estimate C^0_X, the original signal, given C^0_Y, the observed signal at the finest resolution and the degradation model (2). C^0_X cannot be estimated exactly and hence we estimate C^0_X such that the following, $\mathbb{L}^2$ norm, is satisfied

$$\min_{C^0_X} \| C^0_Y - B \otimes C^0_X \|^2 \tag{9}$$

Eq. (2) is always ill-posed [7], which implies there is no unique least-squares norm solution for (9) and hence regularization is essential [20]. So instead of solving (9), we solve a constrained $\mathbb{L}^2$ norm, namely,

$$\min_{C^0_X} [\| C^0_Y - B \otimes C^0_X \|^2 + \lambda^0 F(C^0_X)]. \tag{10}$$

Here, λ^0 is the regularization parameter and $F(\beta)$, captures the characteristics (smoothness for example) of the signal β. The idea of regularization is essentially to restrict the solution space and this makes an ill-posed problem better posed [22]. In signal restoration $F(\cdot)$ usually characterises the smoothness of the signal (see, for example, Eq. (13)).

The idea of signal restoration in a multiresolution framework is *not* to reconstruct X in *one shot* at the finest resolution, but to restore X at different resolutions such that the restored signal at coarse resolution is used in restoring the signal at finer resolutions. In practise, this is achieved by using the restored signal at a coarse resolution to make a *good* initial guess for the next fine resolution. The single most important advantage of using multiresolution framework is computational efficiency [16], in the form of, reduced number of iterations. This motivates us to propose a scheme for signal restoration in a multiresolution framework.

The proposed restoration scheme makes use of the derived relationship (Section 2) between degradation model at different resolutions. Initially, we construct the wavelet transform of the observed signal C^0_Y; for the sake of demonstration, let the wavelet transform (2 levels) of C^0_Y be

$$C^2_{C^1_{C^0_Y}}, \quad D^2_{C^1_{C^0_Y}} \quad \text{and} \quad D^1_{C^0_Y}.$$

The signal restoration is carried out at all resolutions (in this case 2,1,0). At the coarsest resolution (superscript 2) we minimise

$$\left\| \left[C^2_{C^1_{C^0_Y}} \right] - \left\{ B \otimes \left[\overbrace{\overbrace{C^2_{C^1_{C^0_X}} \ \underline{C^2_{\overline{C^1_{C^0_X}}}}} \ \overbrace{\underline{C^2_{C^1_{\overline{C^0_X}}} \ C^2_{\overline{C^1_{\overline{C^0_X}}}}}}} \right] \downarrow 2^2 \right\} \right\|^2 + \lambda^2 F\left(C^2_{C^1_{C^0_X}} \right). \tag{11}$$

The minimisation can be carried out using different iterative restoration algorithms that exist in literature [3,7].

$$C^1_{C^0_X}$$

is obtained from the estimated

$$C^2_{C^1_{C^0_X}}$$

and the available difference signal

$$D^2_{C^1_{C^0_Y}}$$

using the inverse wavelet transform. Now, using the estimated $C^1_{C^0_X}$ as the initial estimate we minimise

$$\left\| C^1_{C^0_Y} - \left[\left\{ B \otimes \left[\overbrace{C^1_{C^0_X}, \underline{C^1_{\overline{C^0_X}}}} \right] \right\} \downarrow 2^1 \right] \right\|^2 + \lambda^1 F\left(C^1_{C^0_X} \right). \tag{12}$$

This procedure is continued till we reach the finest resolution to obtain C^0_X (Algorithm 1).

4. Experimental results

We address two issues, (i) the validity of the degradation model at different resolutions, in essence we check the validity of Eqs. (3) and (5) and (ii) the applicability and computational advantage of using the multiresolution restoration scheme as described in Algorithm 1. In all our simulations, where ever applicable and if not stated otherwise, we use the following:

- Daubechies 4 tap filter [6] for wavelet transform,
- $B = [\frac{1}{3}\ \frac{1}{3}\ \frac{1}{3}]$,
- if X is the signal and $\hat{X}$ is its estimate then, SNR $\stackrel{\text{def}}{=} 10 \times \log_{10}(\|X\|^2/\|X - \hat{X}\|^2)$,
- simulated annealing algorithm [1] for minimisation,[1]
- $\lambda^m = 1$; for $m = 0,1,2,\ldots,k$,
- $F(\beta)$, the constraining function for a signal β of length 2^n was

$$F(\beta) \stackrel{\text{def}}{=} \sum_{i=1}^{2^n} (\beta_i - \beta_{i-1})^2. \tag{13}$$

Algorithm 1: Multiresolution signal restoration.

1: Obtain the wavelet transform of C_Y^0: $C^{\eta}_{C^{\eta-1}_{\ddots_{C^1_{C^0_Y}}}}$, $D^{\eta}_{C^{\eta-1}_{\ddots_{C^1_{C^0_Y}}}}$, $\ldots, D^2_{C^1_{C^0_Y}}$ and $D^1_{C^0_Y}$

2: **for** $k = \eta$ to $k = 1$ (steps of -1) **do**

3: minimise

$$\left\| \left[C^k_{C^{k-1}_{\ddots_{C^1_{C^0_Y}}}} \right] - \left\{ B \otimes \left[\overbrace{\overbrace{C^k_{C^{k-1}_{C^{k-2}_{\ddots_{C^1_{C^0_X}}}}} \quad C^k_{C^{k-1}_{C^{k-2}_{\ddots_{C^1_{C^0_X}}}}}} \cdots \overbrace{C^k_{C^{k-1}_{C^{k-2}_{\ddots_{C^1_{C^0_X}}}}} \quad C^k_{C^{k-1}_{C^{k-2}_{\ddots_{C^1_{C^0_X}}}}}}} \right] \right\} \downarrow 2^k \right\|^2 + \lambda^k F\left(C^k_{C^{k-1}_{C^{k-2}_{\ddots_{C^1_{C^0_X}}}}} \right)$$

4: estimate $C^k_{C^{k-1}_{C^{k-2}_{\ddots_{C^1_{C^0_X}}}}}$.

5: Construct $C^{k-1}_{C^{k-2}_{\ddots_{C^1_{C^0_Y}}}}$ using the inverse wavelet transform with $D^k_{C^{k-1}_{\ddots_{C^1_{C^0_Y}}}}$ as the difference signal and estimated $C^k_{C^{k-1}_{\ddots_{C^1_{C^0_X}}}}$.

6: $C^{k-1}_{C^{k-2}_{\ddots_{C^1_{C^0_X}}}}$ is used as the initial estimate for the next resolution $(k-1)$

7: **end for**

8: At finest resolution — output C_X^0 as the restored signal

4.1. Validation of degradation model at coarse resolutions

Figs. 1–3 aid in demonstrating the validity of the derived relationship between the model at coarse resolution, given the model at a fine resolution (Section 2). Fig. 1 shows the original (C_X^0) and the observed signal (C_Y^0) which was obtained with additive Gaussian noise with zero mean and variance 0.3 after being

[1] One could use any other minimisation scheme.

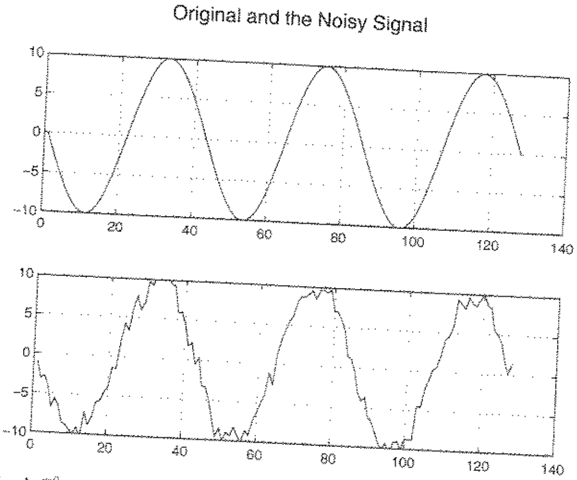

Fig. 1. Original C_X^0 (top), C_Y^0 (bottom) obtained using blur kernel B and $W = N(0,0.3)$.

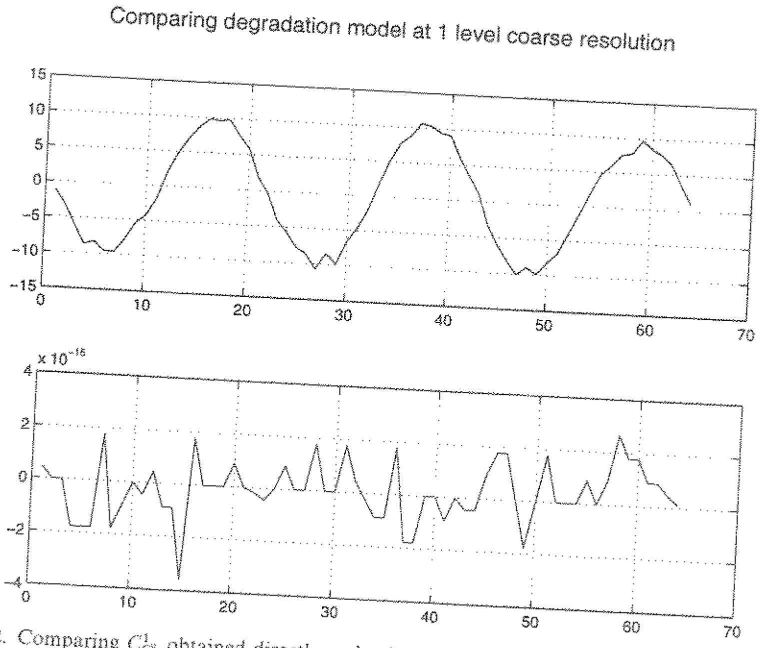

Fig. 2. Comparing $C^1_{C^0_Y}$ obtained directly and using RHS of (3) and the error plot (bottom).

blurred by B. Figs. 2 and 3 capture the degradation model at resolutions $k = 1$ (Eq. (3)) and $k = 2$ (Eq. (5)), respectively. Fig. 2 compares the wavelet transform of the signal C_Y^0 calculated directly from C_Y^0 and $C^1_{C^0_Y}$ calculated using RHS of (3). Observe that the $C^1_{C^0_Y}$ estimated directly and that estimated using the RHS of (3) are almost identical as one would expect and Fig. 2 (bottom), plots the error. The signal and noise power at one level coarse resolution is 315.28 and 0 dB, respectively. Fig. 3 compares the estimate of

$C^2_{C^1_{C^0_Y}}$

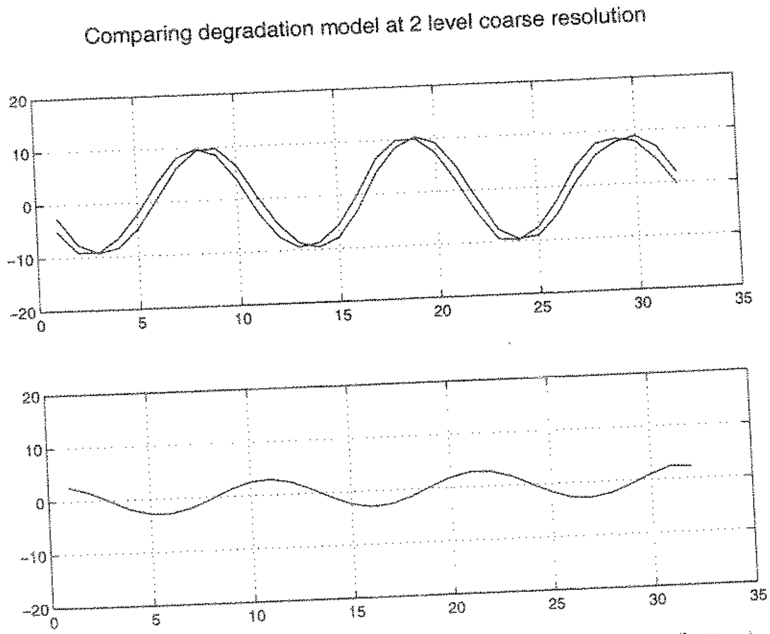

Fig. 3. $C^2_{C^1_{C^0_Y}}$ obtained directly and using RHS of (5) and the error plot (bottom).

using RHS of (5) and estimate of

$$C^2_{C^1_{C^0_Y}}$$

obtained directly from C^0_Y. Fig. 3 (bottom) plots the error between the two estimates. At resolution $k = 2$, the signal power is 50.99 and the noise power is 4.22. The degradation model approximation detoriates in phase and not so much in magnitude (Fig. 3) as we look at further coarse resolutions.

4.2. Application to signal restoration

In this section, we present results which (i) demonstrate the use and applicability of the proposed multiresolution based signal restoration algorithm to restore degraded signals and (ii) compare it with the restored signal obtained working at single resolution (monoresolution) to show computational efficiency of the procedure motivated in Section 3 and described in Algorithm 1.

4.2.1. 1-D signal restoration

Fig. 4(a) is the plot of an original signal and the blur + noisy signal is shown in Fig. 4(b) which has a SNR of 17.28 dB. Fig. 5(a) shows the restored signal after 5000 iterations working at a single (finest) resolution. The error in estimating C^0_X working at a single resolution is shown in Fig. 5(b). The SNR of the restored signal is 22.33 dB.

Fig. 6 shows the restoration obtained using the procedure described in Algorithm 1 with $\eta = 1$. Fig. 6(a) is the restored signal at $k = 1$ after 30 iterations, and Fig. 6(b) is the restored signal at the finest resolution ($k = 0$), with SNR 22.82 dB. At the finest resolution, the restored signal at $k = 1$ (Fig. 6(a)) is used as an initial estimate as described in Algorithm 1. The total number of iterations was 30 at coarse resolution ($k = 1$) and 500 at finest resolution. It can be observed that the SNR of the restored signal (22.82 dB) using multiresolution is slightly better than the SNR obtained using monoresolution (22.33 dB). The main advantage however

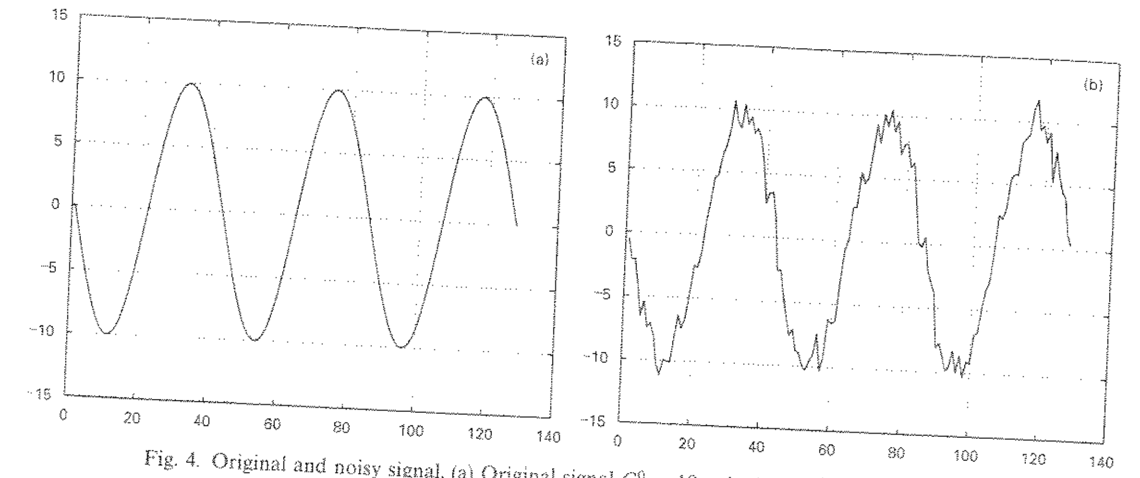

Fig. 4. Original and noisy signal. (a) Original signal $C_X^0 = 10 \times \sin(t)$. (b) $C_Y^0 = B \otimes C_X^0 + C_W^0$.

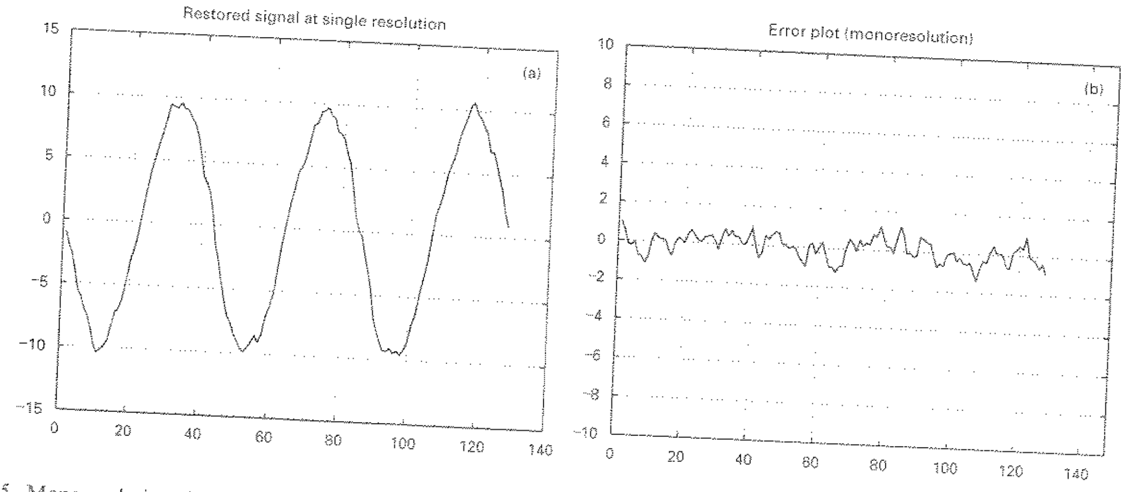

Fig. 5. Monoresolution: Restored signal and error in estimation of C_X^0. (a) Restoration at single (mono) resolution. (b) Error in estimation of C_X^0 (mono).

of using a multiresolution scheme is the computational efficiency in the form of reduced number of iterations. The number of iterations required to obtain the restored signal is 530 for the multiresolution case and 5000 iterations for the monoresolution case. The total time[2] taken for the monoresolution case is about 1235 s compared to 570 s for the multiresolution case, it should be noted that there is extra computation involved (calculation of

$$\left[\overbrace{C^1_{C^0_X}, C^1_{\overline{C^0_X}}}\right],$$

[2] Using Matlab on Sun Ultra 5 in a multiuser environment.

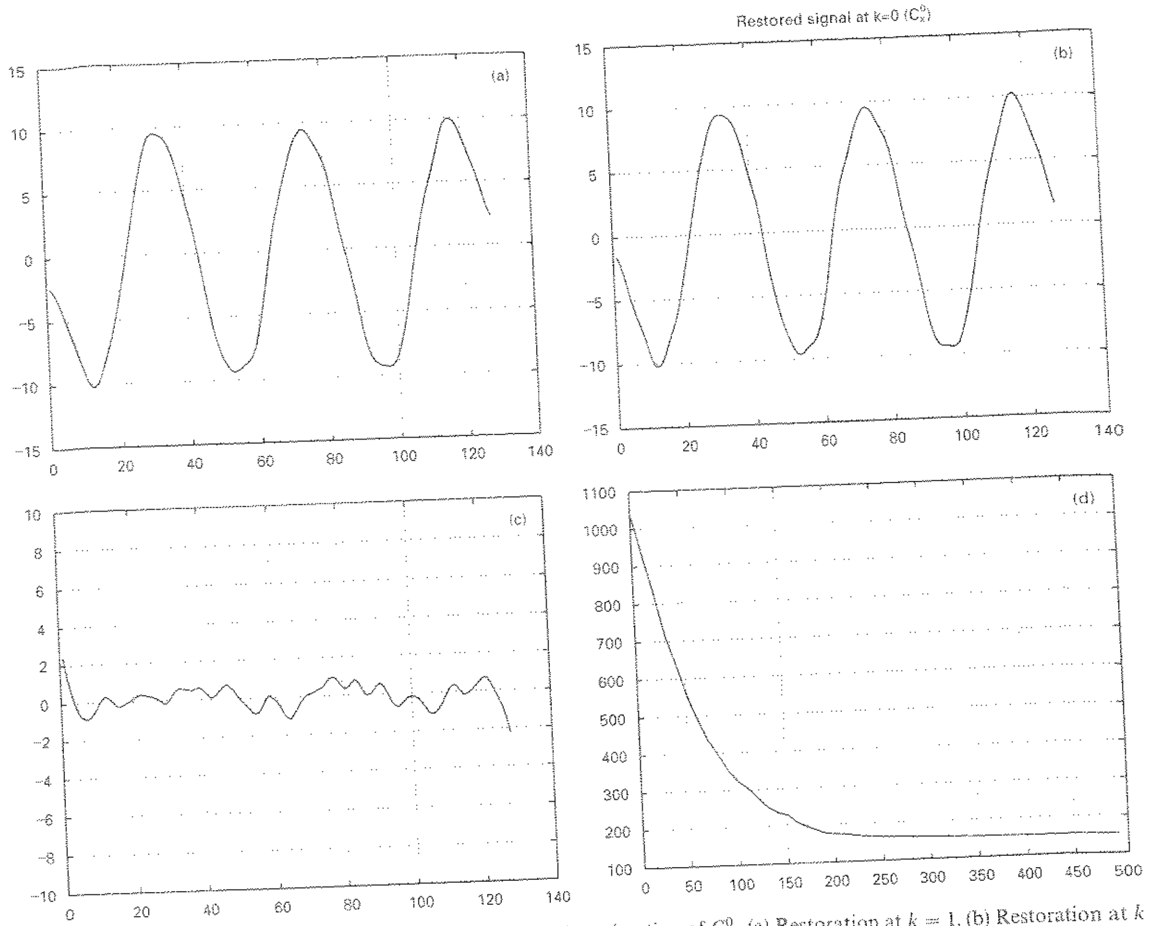

Fig. 6. Multiresolution: restoration using Algorithm 1 and error in estimation of C_X^0. (a) Restoration at $k = 1$. (b) Restoration at $k = 0$, using (Fig. 6(a)). (c) Error in estimation of C_X^0 (multiresolution). (d) Error in estimation of C_X^0 versus iteration.

for example) in restoring signal at coarse resolution, but still there is a factor of 2 improvement in the computational time, which is significant. This demonstrates experimentally that the use of multiresolution makes the algorithm computationally efficient while not sacrificing the final outcome (compare the SNR). Fig. 6(d) shows the converges of the error in estimation of C_X^0 at each iteration at the fine resolution ($k = 0$).

4.2.2. 2-D signal restoration

Fig. 7 shows simulation results for 2D signals. Fig. 7(a) is the original signal of size 128×128 and Fig. 7(b) is the observed signal (blurred + noisy). The SNR of the noisy signal is 20.39 dB. Fig. 7(c) gives the restored signal obtained at the single finest resolution after 25 iterations and Fig. 7(d) gives the signal restored at resolutions 1 (25 iterations) and 0 (3 iterations), using the algorithm proposed in this paper. Note that the restorted image at the coarse resolution (64×64) was used to initialise the restoration at the fine resolution (128×128) resulting in reduced number of iterations at the fine resolution. In our implementation each iteration at coarse resolution was ≈ 10 times faster than each iteration at fine resolution. While both the schemes did not differ significantly in terms of the restored image SNR (22.19 dB for mono

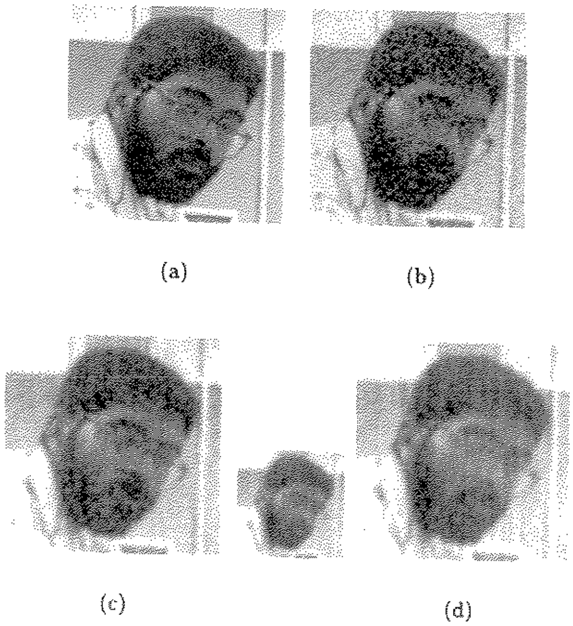

Fig. 7 . Signal restoration for 2-D signals.

and 21.59 dB for multiresolution), the multiresolution based scheme was ≈ 4 times[3] faster than the monoresolution scheme.

Fig. 8(a) is a 64×64 synthetically generated image and Fig. 8(b) shows the image blurred with a Gaussian kernel ($\mathscr{G}$) of size 5×5

$$\mathscr{G} = \begin{bmatrix} 0.003 & 0.013 & 0.022 & 0.013 & 0.003 \\ 0.013 & 0.060 & 0.098 & 0.060 & 0.013 \\ 0.022 & 0.098 & 0.162 & 0.098 & 0.022 \\ 0.013 & 0.060 & 0.098 & 0.060 & 0.013 \\ 0.003 & 0.013 & 0.022 & 0.013 & 0.003 \end{bmatrix}.$$

The observed image (Y) is shown in Fig. 8(c) which has been blurred using a Gaussian kernel ($\mathscr{G}$) and with additive noise (Gaussian with mean 0 and variance 20). The SNR of the blurred and noisy image (Fig. 8(c)) is 8.87 dB. The final restored image is shown in Fig. 8(d) was obtained using the Algorithm described in this paper. The restored image has a SNR of 14.90 dB and was obtained after 25 iterations at resolution 1 and 3 iterations at the fine resolution 0.

5. Conclusion

In this paper we have derived a relationship between the degradation model at different resolutions and have suggested a procedure to construct the degradation model at a coarse resolution from fine resolution.

[3] Compare 25 for monoresolution with $25/10 = 2.5$ (for coarse resolution) $+ 3$ (for fine resolution) $= 5.5$ for the multiresolution case.

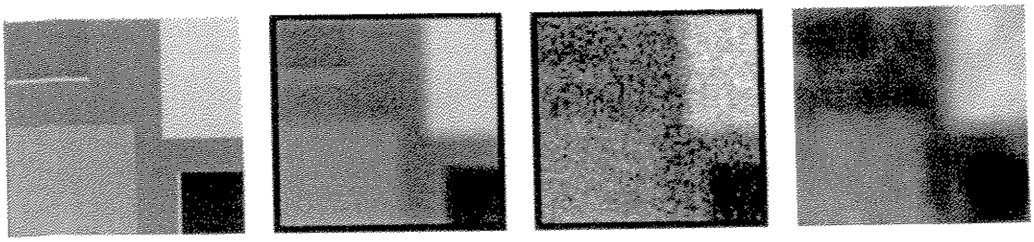

(a) (b) (c) (d)

Fig. 8. Restoration using Gaussian blur and noise.

We show the use and applicability of the knowledge of the relationship between the degradation model at different resolutions by proposing a signal restoration scheme in a multiresolution framework. We substantiated the usefulness, in terms of computational gain, of such a multiresolution restoration scheme through experimental results, for both 1-D and 2-D signals.

Appendix A

Given

$$C_Y^0 = B \otimes C_X^0 + C_W^0 \tag{A.1}$$

at resolution 0, we show that the imaging model takes the form

$$C^1_{C_Y^0} = \left[\left\{ B \otimes \left[\overbrace{C^1_{C_X^0}, \underline{C^1_{\overline{C_X^0}}}} \right] \right\} \downarrow 2^1 \right] + C^1_{C_W^0} \tag{A.2}$$

at one level coarse resolution, namely at resolution 1 in two ways.

Let $B = [b_0, b_1, b_2, \ldots, b_{2k}]$, be a vector of length $(2k+1)$ and let C_Y^0, C_X^0 be vectors of length 2^n, namely, $C_Y^0 = [Y_0, Y_1, Y_2, \ldots, Y_{2^n-1}]^{\mathrm{T}}$ and $C_X^0 = [X_0, X_1, X_2, \ldots, X_{2^n-1}]^{\mathrm{T}}$.

Observe that $B \otimes X$ can be equivalently written in a matrix form as $\mathscr{B}X$, where

$$\mathscr{B} = \underbrace{\begin{bmatrix} b_{2k} & 0 & 0 & \cdots & b_0 & b_1 & \cdots & b_{2k-1} \\ b_{2k-1} & b_{2k} & 0 & \cdots & 0 & b_0 & \cdots & b_{2k-2} \\ \ddots & \ddots & \ddots & \ddots & \ddots & \ddots & \ddots & \ddots \\ b_1 & b_2 & \cdots & b_{2k} & 0 & \cdots & 0 & b_0 \\ \ddots & \ddots & \ddots & \ddots & \ddots & \ddots & \ddots & \ddots \\ 0 & 0 & 0 & \cdots & b_0 & b_1 & \cdots & b_{2k} \end{bmatrix}}_{2^n \times 2^n} \tag{A.3}$$

Let

$$\mathscr{C} = \underbrace{\begin{bmatrix} c_0 & c_1 & c_2 & c_3 & 0 & 0 & \cdots & 0 \\ 0 & c_0 & c_1 & c_2 & c_3 & 0 & \cdots & 0 \\ 0 & 0 & c_0 & c_1 & c_2 & c_3 & \cdots & 0 \\ \ddots & \ddots & \ddots & \ddots & \ddots & \ddots & \ddots & \ddots \\ c_3 & 0 & 0 & \cdots & 0 & c_0 & c_1 & c_2 \\ c_2 & c_3 & 0 & 0 & \cdots & 0 & c_0 & c_1 \\ c_1 & c_2 & c_3 & 0 & \cdots & 0 & 0 & c_0 \end{bmatrix}}_{2^n \times 2^n} \tag{A.4}$$

be the kernel that produces the undecimated wavelet transform. The wavelet transform is obtained by subsampling, namely, $C^1_{C^0_X} = \{\mathscr{C}(X)\}\downarrow 2$. Observe that

$$\mathscr{B}(\mathscr{C}X) = B \otimes \left[\overbrace{C^1_{C^0_X}, C^1_{\overline{C^0_X}}}\right] \tag{A.5}$$

we can write Eq. (A.1) (which is given) as

$$\mathscr{C}(Y)\downarrow 2 = \mathscr{C}(\mathscr{B}X)\downarrow 2 + \mathscr{C}(W)\downarrow 2$$

and we can write Eq. (A.2) as

$$\mathscr{C}(Y)\downarrow 2 = \mathscr{B}(\mathscr{C}X)\downarrow 2 + \mathscr{C}(W)\downarrow 2.$$

Let

$$\begin{aligned} T_1(X) &\stackrel{\text{def}}{=} \mathscr{B}(\mathscr{C}X), \\ T_2(X) &\stackrel{\text{def}}{=} \mathscr{C}(\mathscr{B}X). \end{aligned} \tag{A.6}$$

Observe that the equivalence of (A.1) and (A.2) is established by showing that $T_1 = T_2$:

$$\begin{aligned} T_1 &= \mathscr{B}\mathscr{C} \\ &= \begin{bmatrix} \sum_{j=0}^{3} c_j b_{2k-j} & \sum_{j=0}^{3} c_j b_{2k-j+1} & \cdots & \sum_{j=0}^{3} c_j b_{2k-j-1} \\ \sum_{j=0}^{3} c_j b_{2k-j+1} & \ddots & & \\ \vdots & & \ddots & \\ \sum_{j=0}^{3} c_j b_{2k-j-1} & & \cdots & \sum_{j=0}^{3} c_j b_{2k-j} \end{bmatrix} \\ &= \mathscr{C}\mathscr{B} \\ &= T_2 \end{aligned} \tag{A.7}$$

This completes the proof. □

References

[1] E. Aarts, J. Korst, Simulated Annealing and Boltzmann Machines, Wiley, New York, 1989.

[2] L. Alvarez, L. Mazorra, Signal and image restoration using shock filters and anisotropic diffusion, J. Numer. Anal. 31 (2) (1994) 590–605.

[3] M.R. Bhatt, U.B. Desai, Robust image restoration algorithm using Markov random field mode, CVGIP: Graphical Models Image Process. 56 (1) (January 1994) 61.

[4] B.S. Chen, C.W. Lin, Multiscale Wiener filter for the restoration of fractal signals: wavelet filter bank approach, IEEE Trans. Signal Process. 42 (1994) 2972–2982.

[5] M.-H. Chen, T. Pavlidis, Restoration of blurred bilevel signals by multiscaling with finite support filters, Proceedings 11th IAPR International Conference on Pattern Recognition 1992, pp. 632–634.

[6] I Daubechies, Ten Lectures on Wavelets, SIAM, Philadelphia, PA, 1992.

[7] A.K. Katsaggelos, Digital Image Restoration, Springer, Berlin, 1991.

[8] A.J. Levy, A fast quadratic programming algorithm for positive signal restoration, IEEE Trans. Acoust. Speech Signal Process. 31 (1983) 1337–1341.

[9] S.Z. Li, MRF Modeling in Computer Vision, Springer, Tokyo, 1995.

[10] H. Maitre, A general scheme for signal restoration with application to picture processing, Pattern Recognition Image Process. 5 (1981) 430–432.

[11] E.L. Miller, Efficient computational methods for wavelet domain signal restoration problems, IEEE Trans. Signal Process. 47 (April 1999).

[12] P.K. Nanda, K. Sunil Kumar, S. Ghokale, U.B. Desai, A multiresolution approach to color image restoration and parameter estimation using homotopy continuation method, Proceedings International Conference on Image Processing, 1995.

[13] G. Nicholls, M. Petrou, On multiresolution image restoration, International Conference on Pattern Recognition, 1994, pp. 63–67.

[14] E. Oja, H. Ogawa, Parametric projection filter for image and signal restoration, IEEE Trans. Acoust. Speech Signal Process. 34 (1986) 1643–1653.

[15] S. Ranganath, Image filtering using multiresolution representations, IEEE Trans. Pattern Anal. Mach. Intell. 13 (1991) 426–440.

[16] A. Rosenfeld, Multiresolution Image Processing and Analysis, Springer, Berlin, 1984.

[17] J.L.C. Sanz, T.S. Huang, Iterative time-limited signal restoration, IEEE Trans. Acoust. Speech Signal Process. 31 (1983) 643–650.

[18] J.L.C. Sanz, T.S. Huang, A unified approach to noninterative linear signal restoration, IEEE Trans. Acous. Speech Signal Process. 32 (1984) 403–409.

[19] G. Sharma, H.J. Trussell, Set theoretic signal restoration using an error in variables criterion, IEEE Trans. Image Process. 6 (12) (December 1997) 1692–1697.

[20] J.-L. Starck, F. Murtagh, A. Bijaoui, Image restoration with denoising using multiresolution, in: R.J. Hanisch, R.L. White (Eds.), The Restoration of HST images and Spectra II, Space Telescope Science Institute, 1993, pp. 111–117.

[21] K. Sunil Kumar, U.B. Desai, Joint segmentation and image interpretation, Pattern Recognition 32 (April 1999) 557–589.

[22] D. Terzopoulos, Image analysis using multigrid relaxation methods, IEEE Trans. Pattern Anal. Mach. Intell. 8 (1986) 129–138.

[23] H.J. Trussell, M.R. Civankr, The feasible solution in signal restoration, IEEE Trans. Acoust. Speech Signal Process. 32 (1984) 201–212.

[24] J.K. Tugnait, Constrained signal restoration via iterated extended Kalman filtering, IEEE Trans. Acoust. Speech Signal Process. 33 (1985) 472–475.

[25] Y.F.I. Wong, Nonlinear scale space filtering and multiresolution system, IEEE Trans. Image Process. 4 (1995) 774–787.